

Three-Dimensional Heat Conduction in multi-connected domains using GFEM with hexaedrals of 27 nodes

Estaner Claro Romão, Jairo Aparecido Martins, Luiz Felipe Mendes de Moura

Abstract - A numerical solution for temperature profile in three-dimensional heat conduction inside multi-connected geometry is presented. The special discretization has been done by Galerkin Finite Element Method (GFEM). Four applications are presented to demonstrate the efficiency of the proposed method. Of these, the first two use a doubly connected domain, and the other, a multi-connected domain, and the first and the third used to validate the results in their respective fields through the analytical solution. To analyze the results, the norms of the errors and their graphs are studied.

Keywords - Finite Element Method, Galerkin Finite Element Method, heat conduction, multi-connected domains.

I. INTRODUCTION

Since the early '50s, many researchers have used the Finite Element Method (FEM) in many applications, detaching the pioneering papers of [1,3], which made use of the method in structural analysis. Some decades later [4,7] successfully used this formulation in problems involving heat conduction, since that, when applied to problems governed by self-adjoint elliptic or parabolic partial differential equations, the Galerkin Finite Element Method (GFEM) leads to symmetric stiffness matrices.

Estaner Claro Romão works in Federal University of Itajubá, Campus of Itabira. 35900-373, Itabira, Minas Gerais, Brasil. Email: estanerromao@unifei.edu.br

Jairo Aparecido Martins works in Department of Product Engineering, Metso Minerals, Av. Independência, 2500, Iporanga, 18087-501, Sorocaba, São Paulo, Brasil. E-mail: jairophd@ig.com.br

Luiz Felipe Mendes de Moura works in Mechanical Engineering College, Department of Thermal and Fluids. State University of Campinas. 13083-860, Campinas, São Paulo, Brasil. Email: felipe@fem.unicamp.br

Recently, several authors have presented applications of the finite element method for two and tridimensional problems, among them [8,11].

Also noteworthy is the two-dimensional study of heat conduction in multiply connected domains carried by [10], extended to three-dimensional case in this work that presents a numerical solution to the heat conduction in solids with doubly connected domains using the GFEM.

It is important argue that the main objective this paper is the application of the proposed method in tri-dimensional domain multi-connected, once to simple domain, like in cubes [12] it was already done. Despite the domains are multi-connected, the meshes chosen to this work are uniform, and due to the paper aiming is to allow other authors to compare their results.

In order to analyze the accuracy of the methodology adopted, it is used the norm L_2 , which represent the average error in all domain, and the norm L_∞ , that represents the highest error in all domain, in analyzes of the application 1 and 3, which already have the analytical solution proposed.

II. MODEL EQUATION

Considering the tridimensional heat conduction equation in closed limited solid domains designed as $\Omega \subset \mathcal{R}^3$, the model equation has the following form:

$$k_x \frac{\partial^2 T}{\partial x^2} + k_y \frac{\partial^2 T}{\partial y^2} + k_z \frac{\partial^2 T}{\partial z^2} + BT = 0 \quad (1)$$

where is a function dependable of spatial coordinates, k_x , k_y e k_z being the thermal conductivity in each direction, here considered

constant. Few after, it is presented a brief of spatial discretization, more details are found in [12].

III. SPATIAL DISCRETIZATION

Here, the GFEM is applied for discretization of the integral equations. In this method an approximation of unknown variable is a function \hat{T} that when substituted in the Eq. (1) produces a null residual. So, the approximation form is:

$$T \approx \hat{T}^e = \sum_{j=1}^{N_{nodes}} N_j \hat{T}_j^e \tag{2}$$

where N_{nodes} is the number of nodes of each element, N_j are the function of interpolation and \hat{T}_j^e the nodal values of T in the element. The residue is determined by the replacement of the approximation \hat{T} in Eq. (1), and is defined as:

$$R = k_x \frac{\partial^2 \hat{T}}{\partial x^2} + k_y \frac{\partial^2 \hat{T}}{\partial y^2} + k_z \frac{\partial^2 \hat{T}}{\partial z^2} + BT \tag{3}$$

The solution is found by forcing the pondered residual to be null. In other words, it must be found as a function of $\hat{T}^e \in V^e$, $V^e \in C^2(\Omega)$, such as:

$$\int_{\Omega^e} R v_i^e d\Omega = 0, \forall v_i^e \in V^e, i = 1, 2, \dots, N_{nodes} \tag{4}$$

In the GFEM, the weight function is the same interpolation function, i.e. $v_i^e = N_i$, $i = 1, 2, \dots, N_{nodes}$. After integration of Eq. (4) the result is an algebraic system of equations written in matricial form as follow:

$$[K] \{ \hat{T} \} = \{ F_i \} \tag{5}$$

in which the matrix coefficients are,

$$K_{ij} = \int_{\Omega^e} BN_i N_j d\Omega - \int_{\Omega^e} k_x \frac{\partial N_i}{\partial x} \frac{\partial N_j}{\partial x} d\Omega - \int_{\Omega^e} k_y \frac{\partial N_i}{\partial y} \frac{\partial N_j}{\partial y} d\Omega - \int_{\Omega^e} k_z \frac{\partial N_i}{\partial z} \frac{\partial N_j}{\partial z} d\Omega \tag{6}$$

e

$$F_i = \int_{\Gamma_q} N_j (q + h(T - T_a)) d\Gamma_q \tag{7}$$

with $i, j = 1, 2, \dots, N_{nodes}$, T_a the temperature of the environment, h the heat transference coefficient, q the flux of heat in the contour and Γ_q the contour where none temperature is described.

IV. NUMERICAL APPLICATIONS

The system of algebraic equations represent by Eq. (5) was solved by the Gauss-Seidel method and stop criteria with maximum error $E_{max} \leq 10^{-10}$. The computational code was developed in FORTRAN language and the meshes were refined until the limit of the computer's memory capacity. Linear hexahedra with eight nodes were used, with h representing the size of the element (cubic element).

The L_2 norm of the error was defined like in [13]:

$$\|e\| = \left[\left(\sum_{i=1}^{N_{n\text{ost}}} e_i^2 \right) / N_{n\text{ost}} \right]^{1/2}, \text{ being } N_{n\text{ost}} \text{ the total}$$

number of nodes in the mesh and $e_i = |T_{(\text{num})_i} - T_{(\text{an})_i}|$, where $T_{(\text{num})}$ is the result from the numerical solution and $T_{(\text{an})}$ is the result from the analytical solution, respectively, and the L_∞ norm, defined by $\|e\|_\infty = |T_{(\text{num})} - T_{(\text{an})}|$, which is the maximum error in the entire domain.

In the following, two numerical applications are presented, using the same domain (Fig. 1). At the first, it used an analytical solution to validate the computational code at this type of domain. In the two last applications is considered a domain multi-connected (Fig. 5), while in the third an analytical solution is utilized to validate the computational code.

Application 1

In this application is adopted an analytical solution for the Eq. (1) with k_x , k_y , k_z and B in an unity manner, as follow;

$$T(x, y, z) = \text{sen } x + \text{sen } y + \text{sen } z, \\ \frac{\partial T(x, y, z)}{\partial x} = \cos x, \quad \frac{\partial T(x, y, z)}{\partial y} = \cos y, \\ \frac{\partial T(x, y, z)}{\partial z} = \cos z.$$

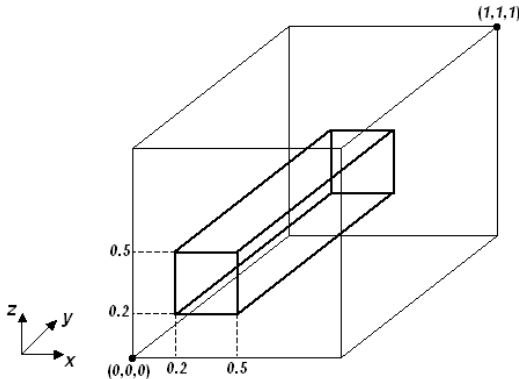


Fig. 1 Cubic doubly connected domain.

and the boundary conditions of first type, defined by the own analytical solution.

Here, the precision of GFEM is analyzed towards Norms L_2 and L_∞ , which are shown in the Tables 1 and 4, considering $h = \Delta x = \Delta y = \Delta z$, being $h = \Delta x = \Delta y = \Delta z$ the edges in the three directions and Nelem the number of elements in the mesh. Figure 2 shows the mesh in the plane xz and $y = 0.1$, with $h = 1/20$, being the mesh generated internally in the computational code.

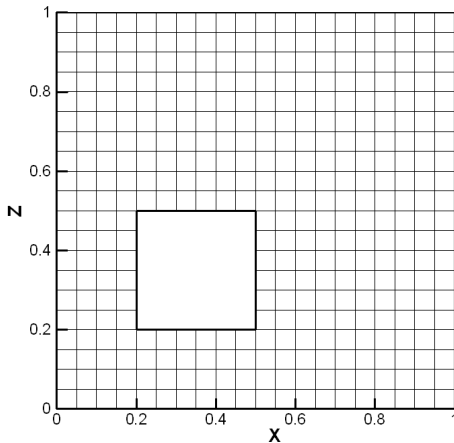


Fig. 2 Mesh in the plane xz with $y = 0.1$, $h = 1/20$.

In Table 1 is verified with the mesh slightly refined, $h = 1/10$ that the GFEM already reaches, in the two norms proposed, an accuracy of order 10^{-5} . Applying several refinements in the mesh, reaching till $h = 1/60$, is observed that the refinement is not yet necessary, once the accuracy advantage is too small to hexahedron with 8 nodes. On the other hand, it is remarkable by the Table 3 that the refinement of the mesh

for hexahedron with 27 nodes starts to become harmful to the method accuracy.

Table 1. Norm of error in the solution of $T(x,y,z)$, application 1.

8 nodes				
NNost	h	Nelem	Norm L_2	Norm L_∞
1287	1/10	910	1.59E-05	4.87E-05
8736	1/20	7280	4.33E-06	1.22E-05
27807	1/30	24570	2.03E-06	5.65E-06
63960	1/40	58240	1.24E-06	3.48E-06
122655	1/50	113750	9.22E-07	2.63E-06
209352	1/60	196560	7.93E-07	2.34E-06

A special contribution given by this paper is the analyzes of Norms L_2 and L_∞ in terms of error of numerical solution of the initials derivatives of T (Tables 2 and 4). This result is of extreme importance in heat transfer problems, making possible the analyses of the heat flux in any point within the domain. In GFEM, the proceeding used is similar of the approximation presented in Eq. (2):

Table 2. Norm of error in the solution of $T_x(x,y,z) = T_y(x,y,z) = T_z(x,y,z)$, aplicação 1.

8 nodes				
NNost	h	Nelem	Norm L_2	Norm L_∞
1287	1/10	910	2.57E-02	4.14E-02
8736	1/20	7280	1.31E-02	2.08E-02
27807	1/30	24570	8.80E-03	1.39E-02
63960	1/40	58240	6.62E-03	1.04E-02
122655	1/50	113750	5.31E-03	8.39E-03
209352	1/60	196560	4.43E-03	7.00E-03

$$\frac{\partial T}{\partial x_k} \approx \frac{\partial \hat{T}^e}{\partial x_k} = \sum_{i=1}^{Nnodes} \frac{\partial N_i}{\partial x_k} \hat{T}_i^e,$$

where $k = 1, 2$ ou 3 , being $x_1 = x, x_2 = y$ e $x_3 = z$.

In the Table 2, where the hexahedron with eight nodes is utilized, it presents that the previous solution, proposed to the calculus of the derivatives of T obtains results with 3 to 4 orders of accuracy, are smaller than presented in the Table 1, Norms of T . The same happens with the results found in the Table 4, which makes use of hexahedron with 27 nodes, where also, according to the results in the Table 3, the refinement is harmful to the accuracy of the method.

Table 3. Norm of error in the solution of $T(x,y,z)$, application 1.

27 nodes				
NNost	h	Nelem	Norm L_2	Norm L_∞
8736	1/10	910	4.80E-07	3.53E-06
63960	1/20	7280	1.49E-06	1.66E-05
209352	1/30	24570	2.07E-07	1.69E-06

Table 4. Norm of error in the solution of $T_x(x,y,z) = T_y(x,y,z) = T_z(x,y,z)$, application 1.

27 nodes				
NNost	h	Nelem	Norm L_2	Norm L_∞
8736	1/10	910	5.76E-04	9.03E-04
63960	1/20	7280	2.17E-04	2.13E-03
209352	1/30	24570	7.24E-05	3.78E-04

Application 2

In this case, in Eq. (1) are considered k_x, k_y and k_z unities, $B = 0$ and the following boundary condition:

- plane xz with $y = 0$ or $y = 1 \Rightarrow \partial T/\partial y = 0$ (isolated)
- plane yz with $x = 0$ or $x = 1 \Rightarrow T = 5$
- plane xy with $z = 0$ or $z = 1 \Rightarrow T = 5$

- plane yz (hole) with $x = 0.2$ or $x = 0.5 \Rightarrow T = 0$
- plane xy (hole) with $z = 0.2$ or $z = 0.5 \Rightarrow T = 0$

The Figures 3 and 4 demonstrate what was expected physically, it means, a more shrink distribution of temperature in the region of x and $z = 0$ without oscillations and more spaced in the region of x and $z = 1$ (Fig. 3) and a line of flux null in a region on the left from the center of domain (Fig. 4), due to influence of the hole, being at left from the domain.

In the applications 3 and 4, the domain is multi-connected, presenting two holes placed in the plane xz , as seen in the Figure. 5.

Application 3

We analyzed here a problem of heat transferring under a domain multi-connected. In the application 1, the cubic domain presented one hole, (Fig. 1); while here, it is composed by two holes. These are considered k_x, k_y and k_z unities and B null.

To validate the computational code it is used the following analytical solution [14,15],

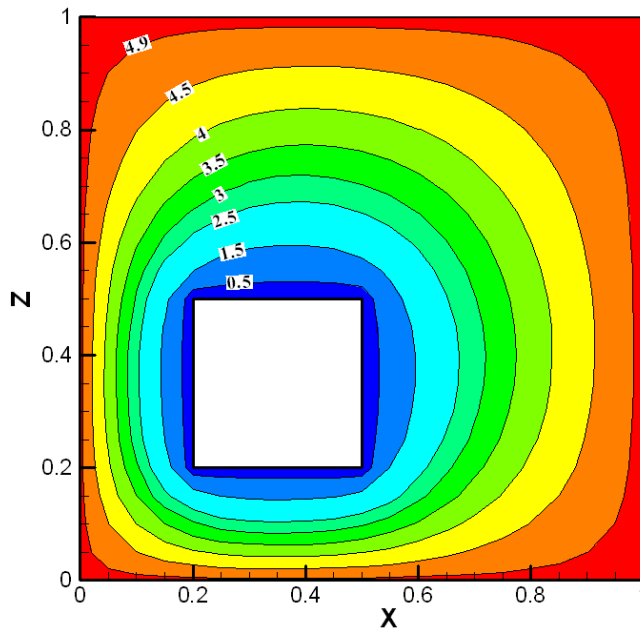


Fig. 3 Profile of $T(x,y,z)$ in the plane xz , with $y = 0.1$ and $h = 1/20$, application 2.

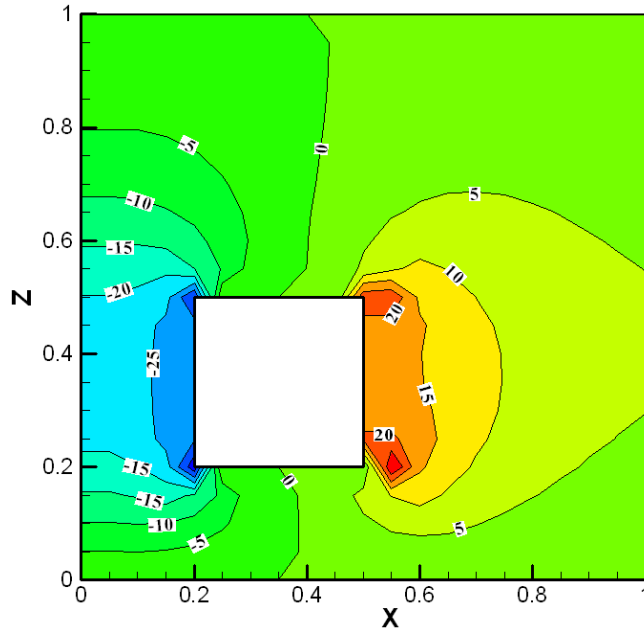


Fig. 4 Profile of $T_x(x,y,z)$ in the plane xz , with $y = 0.1$ and $h = 1/20$, application 2.

$$T(x, y, z) = \frac{\sin(\pi.y)\sin(\pi.z)}{\sinh(\pi\sqrt{2})} \times [2\sinh(\pi\sqrt{2}x) + \sinh(\pi\sqrt{2}(1-x))],$$

$$\frac{\partial T(x, y, z)}{\partial x} = \frac{\sin(\pi.y)\sin(\pi.z)}{\sinh(\pi\sqrt{2})} \times [2\sqrt{2}\pi \cosh(\pi\sqrt{2}x) - \sqrt{2}\pi \cosh(\pi\sqrt{2}(1-x))],$$

$$\frac{\partial T(x, y, z)}{\partial y} = \frac{\pi \cos(\pi.y)\sin(\pi.z)}{\sinh(\pi\sqrt{2})} \times [2\sinh(\pi\sqrt{2}x) + \sinh(\pi\sqrt{2}(1-x))],$$

$$\frac{\partial T(x, y, z)}{\partial z} = \frac{\sin(\pi.y)\pi \cos(\pi.z)}{\sinh(\pi\sqrt{2})} \times [2\sinh(\pi\sqrt{2}x) + \sinh(\pi\sqrt{2}(1-x))].$$

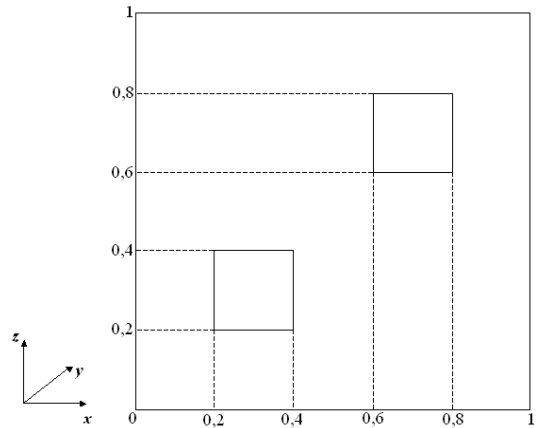


Fig. 5 Cubic Multi-Connected Domain (section xz).

The boundary conditions were chosen to satisfy the analytical solution proposed at this problem.

To the boundary conditions proposed at this application (analytical solution), on contrary of the application 1, it was reached a Norm of error around 10^{-5} only by using a mesh with $h = 1/50$ (Table 5).

Table 5. Norm of error in solution of $T(x,y,z)$, application 3.

8 nodes				
NNost	h	Nelem	Norm L_2	Norm L_∞
1309	1/10	920	1.58E-03	6.64E-03
8883	1/20	7360	4.29E-04	1.64E-03
28241	1/30	24840	1.96E-04	7.32E-04
64903	1/40	58880	1.12E-04	4.12E-04
124389	1/50	115000	7.27E-05	2.63E-04
212219	1/60	198720	5.08E-05	1.83E-04

Table 6. Norm of error in solution of $T_x(x,y,z)$, application 3.

8 nodes				
NNost	h	Nelem	Norm L_2	Norm L_∞
1309	1/10	920	3.62E-01	1.66E+00
8883	1/20	7360	1.88E-01	9.01E-01
28241	1/30	24840	1.27E-01	6.18E-01
64903	1/40	58880	9.58E-02	4.71E-01
124389	1/50	115000	7.69E-02	3.80E-01
212219	1/60	198720	6.42E-02	3.18E-01

In Tables 6 and 7 the same difficulty found in the application 1 is noted, thus, the error in the numerical solution of derivatives presented 2 to 3 orders of accuracy inferior than the solution of T . This situation can be mitigated with a higher refinement in mesh, however a small value to h.

Table 7. Norm of error in the solution of $T_y(x,y,z) = T_z(x,y,z)$, application 3.

8 nodes				
NNost	h	Nelem	Norm L_2	Norm L_∞
1309	1/10	920	2.01E-01	9.78E-01
8883	1/20	7360	9.91E-02	4.92E-01
28241	1/30	24840	6.57E-02	3.28E-01
64903	1/40	58880	4.91E-02	2.46E-01
124389	1/50	115000	3.92E-02	1.97E-01
212219	1/60	198720	3.26E-02	1.64E-01

Table 8. Norm of error in the solution of $T(x,y,z)$, application 1.

27 nodes				
NNost	h	Nelem	Norm L_2	Norm L_∞
8883	1/10	920	2.05E-05	1.90E-04
64903	1/20	7360	2.65E-06	1.76E-05
212219	1/30	24840	4.86E-06	5.01E-06

Table 9. Norm of error in the solution of $T_x(x,y,z)$, application 1.

27 nodes				
NNost	h	Nelem	Norm L_2	Norm L_∞
8883	1/10	920	2.03E-02	1.19E-01
64903	1/20	7360	5.22E-03	3.28E-02
212219	1/30	24840	2.46E-03	1.49E-02

With the usage of hexahedron of 27 nodes (Tables 8, 9 and 10), the Galerkin method already reached an accuracy of 10^{-5} in $T(x,y,z)$ for a mesh with $h = 1/10$, and an accuracy of order 10^{-3} to the derivatives. One important

information is that, with hexahedron of 27 nodes, the lack of accuracy of derivatives in comparison to $T(x,y,z)$ is smaller than the hexahedron with 8 nodes.

Table 10. Norm of error in the solution of $T_y(x,y,z) = T_z(x,y,z)$, aplicação 1.

27 nodes				
NNost	h	Nelem	Norm L_2	Norm L_∞
8883	1/10	920	8.81E-03	5.12E-02
64903	1/20	7360	2.12E-03	1.28E-02
212219	1/30	24840	1.21E-03	9.76E-03

Application 4

In this case, the Eq. (1), it considers k_x, k_y and k_z unities, $B = 0$ and the boundary conditions given by:

- plane xz with $y = 0$ ou $y = 1 \Rightarrow \partial T / \partial y = 0$ (isolated)
- plane yz with $x = 0$ ou $x = 1 \Rightarrow T = 5$
- plane xy with $z = 0$ ou $z = 1 \Rightarrow T = 5$
- plane yz (holes) with $x = 0.2; x = 0.4; x = 0.6$ or $x = 0.8 \Rightarrow T = 0$
- plane xy (holes) with $z = 0.2; z = 0.4; z = 0.6$ or $z = 0.8 \Rightarrow T = 0$

Fig. 6 represents the mesh in the section xz , being this built in a regular manner with hexahedron 8 nodes.

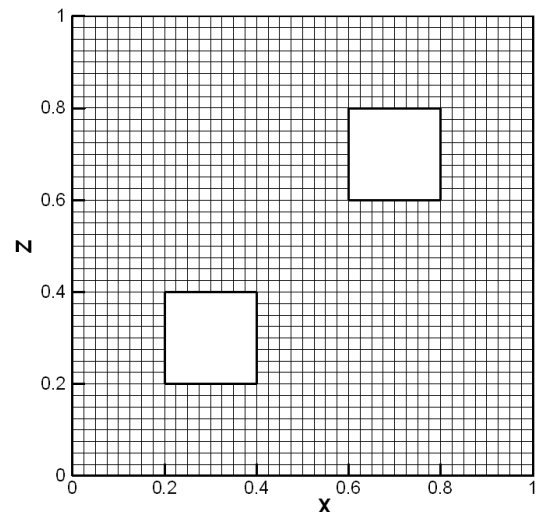


Fig. 6 Mesh in plane xz with $y = 0.1, h = 1/30$, application 4.

The results of the profile of temperatures and its derivative in x and in the plane xz with

$y = 0.1$ are observed in the Figures 7 and 8.

In order to avoid that the analysis of problems with non solution is done again only quantitatively, in Table 1 are shown some points of the mesh and its respective values of temperature.

The mesh was refined in such way to demonstrate that how small is the value of h , smaller is the temperature variation on these points.

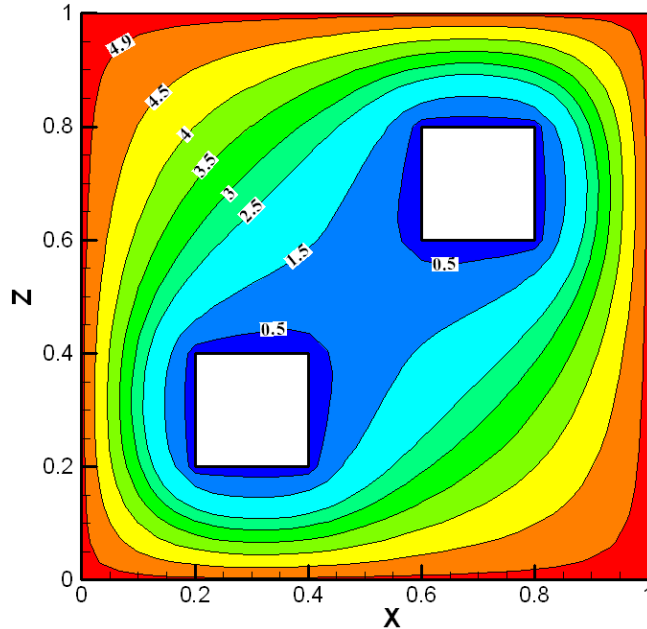


Fig. 7 Profile of $T(x,y,z)$ on plane xz , with $y = 0.1$ and $h = 1/30$, application 4.

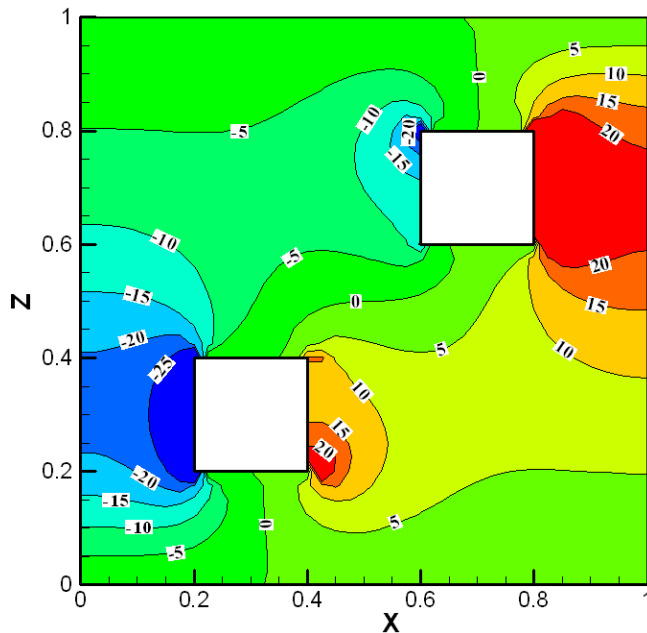


Fig. 8 Profile of $T_x(x,y,z)$ on plane xz , with $y = 0.1$ and $h = 1/30$, application 4.

Table 11. Values of temperature found in some points on the computational mesh.

h	Points					
	x = 0.5 y = 0.5 z = 0.5	x = 0.5 y = 0.1 z = 0.9	x = 0.1 y = 0.1 z = 0.1	x = 0.2 y = 0.4 z = 0.1	x = 0.9 y = 0.3 z = 0.1	x = 0.7 y = 0.6 z = 0.9
1/10	0.855617	3.332209	3.893269	3.073076	4.746810	2.618263
1/20	0.949956	3.410329	3.986353	3.078756	4.745790	2.697934
1/30	0.970967	3.426053	4.003716	3.090993	4.746016	2.713255
1/40	0.979251	3.432008	4.010020	3.096199	4.746201	2.718891
1/50	0.983554	3.435073	4.013191	3.099240	4.746328	2.721745
1/60	0.986140	3.436914	4.015068	3.101176	4.746418	2.723441
1/70	0.987843	3.438127	4.016292	3.102504	4.746483	2.724551
Erro*	1.70E-03	1.21E-03	1.22E-03	1.32E-03	6.50E-05	1.11E-03

* Difference between the results for $h = 1/70$ and $h = 1/60$.

In the Table 6 it is clear that the mesh refinement improve significantly the numerical results. In a mesh with $h = 1/30$, which requires a smaller memory utilization and reduced computational time, it is noted that, among the chosen points, the higher comparative difference among the results with the mesh $h = 1/70$ occurs in the point $(x,y,z) = (0.5;0.5;0.5)$, being around 0.016876, which in real application in engineering is considered neglected.

V. CONCLUSIONS

The GFEM is shown as an excellent tool in the solution of problems of heating conduction in tridimensional domains multi-connected. The results presented in the solution of $T(x,y,z)$ are excellent, but the calculation of derivatives using the finite element have not shown so effective; despite of that, the errors to meshes less refined can be considered acceptable to engineering practices, once those are around 10^{-2} . However it is important to mention that, whether the purpose is to calculate the heat flux, the Galerkin method is advisable with hexahedron of 27 nodes, where the mesh with $h = 1/10$, already reached an accuracy of around 10^{-3} .

ACKNOWLEDGMENTS

This paper is sponsored by the National Council of Scientific and Technological Development – CNPq – Brasil (Proc. 500382/2011-5).

REFERENCES

- [1] Turner, M. J., Clough, R. W., Martin, H. C., and Topp, L. P.. Stiffness and Deflection Analysis of Complex Structures, *Journal of Aerospace Science and Technologies*, vol. 23, n. 9, pp. 805-823, 1956.
- [2] Clough, R.W.. The Finite Element Method in Plane Stress Analysis. In: *Proceedings of 2nd Conf. on Electronic Computation, American Society of Civil Engineers*, 345-378, 1960.
- [3] Argyris, J.H.. *Recent Advances in Matrix Methods of Structural Analysis*. Pergamon Press, 1963.
- [4] Zienkiewicz, O.C. and Cheung, Y.K.. Finite elements in the solution of field problems. *The Engineer*, pp. 507-510, 1965.
- [5] Oden, J.T. and L.C. Wellford, Jr.. Analysis of viscous flow by the finite element method. *AIAA Journal*, v.10, pp. 1590-1599, 1972.
- [6] Chung, T.J.. *Finite Element Analysis in Fluid Dynamics*. McGraw-Hill, 1978.
- [7] Baker, A.J.. *Finite Element Computational Fluid Mechanics*. McGraw-Hill, 1983.
- [8] Camprub, N., Colominas, I., Navarrina, F. and Casteleiro, M.. Galerkin, Least-Squares and G.L.S. numerical approaches for convective-diffusive transport problems in engineering. In: *European Congress on Computational Methods in Applied Sciences and Engineering*, 2000.
- [9] Romão, E.C. ; Moura, L.F.M. and Silva, J.B.C.. Analysis of Error in the Solution of the 2-D Diffusion Equation by Finite Element Methods. *Tendências em Matemática Aplicada e Computacional*, vol. 9, n. 2, pp. 287-298, 2008.
- [10] Romão, E.C., Moura, L.F.M. and Silva, J.B.C.. Heat Transfer in Multi-Connected and Irregular Domains with Non-Uniform Meshes, *Thermal Engineering*, vol. 7, n. 02, p. 44-50, 2008.
- [11] Hannukainen, A, Korotov, S. and Krezek, M., 2010. Nodal $O(h^4)$ -Superconvergente in 3D by averaging piecewise linear, bilinear, and trilinear FE approximations. *Journal of Computational Mathematics*, vol.28, n.1, pp.1-10, 2010.
- [12] Romão, E. C., Campos, M. D., Moura, L. F. M.. Application of Galerkin and Least-Squares finite element method in the solution of 3D Poisson and Helmholtz equations. *Computers & Mathematics with Applications*, vol. 62, p. 4288-4299, 2011.
- [13] Zlhal, M.. Superconvergence and reduced integration in the finite element method. *Mathematics and Computation*, vol. 32, n.143, p. 663-685, 1978.

- [14] Spitz, W. F.; Carey, G. F. A High-Order Compact Formulation for the 3D Poisson Equation. *Numerical Methods for Partial Differential Equations*, vol. 12, p. 235-243, 1996.
- [15] Gupta, M. M.; Kouatchou, J. Symbolic Derivation of Finite Difference Approximations for the Three-Dimensional Poisson Equation. *Numerical Methods for Partial Differential Equations*, vol. 14, n.5, p. 593-606, 1998.